

## Phase diagrams of mixtures of ethyl palmitate with fatty acid ethyl esters

M.C. Costa<sup>a</sup>, L.A.D. Boros<sup>b</sup>, M.L.S. Batista<sup>c</sup>, J.A.P. Coutinho<sup>c</sup>, M.A. Krähenbühl<sup>b</sup>, Antonio J.A. Meirelles<sup>a,\*</sup>

<sup>a</sup>EXTRAE, Department of Food Engineering (DEA) – School of Food Engineering (FEA), University of Campinas (UNICAMP), 13083-862 Campinas, São Paulo, Brazil

<sup>b</sup>LPT, Department of Chemical Processes (DPQ) – School of Chemical Engineering (FEQ), University of Campinas (UNICAMP), 13083-970 Campinas, São Paulo, Brazil

<sup>c</sup>CICECO, Departamento de Química da, Universidade de Aveiro, 3810-193 Aveiro, Portugal

### ARTICLE INFO

#### Article history:

Received 30 August 2010

Received in revised form 28 April 2011

Accepted 15 July 2011

Available online 30 July 2011

#### Keywords:

Cloud point

Fatty acid ethyl ester (FAEE)

Ethyl palmitate

Solid–liquid equilibrium

Predictive UNIQUAC

### ABSTRACT

The cloud point is an important property of biodiesel, controlling its low temperature behaviour, especially the fluidity of the fuel. Although biodiesel is an interesting renewable energy source, data for the melting/cloud point of biodiesel or simple binary or ternary mixtures of fatty acid ethyl esters (FAEE) are still scarce in the literature, particularly for those involving ethyl esters. The phase diagrams of six binary mixtures of ethyl palmitate with saturated and unsaturated fatty acid ethyl esters were determined by Differential Scanning Calorimetry (DSC). The determined systems were successfully described employing the UNIQUAC model. The experimental data indicates that the cloud point is controlled by the fatty acid ethyl ester in the mixture with higher melting temperature.

© 2011 Elsevier Ltd. All rights reserved.

### 1. Introduction

Nowadays, there is a growing interest in biodiesel due to its reduced impact on the environment and to its favourable characteristics as a fuel when compared with petroleum based fuels, such as its biodegradability, non-toxicity, lower emission of pollutants and the fact that it is produced from renewable resources. The use of biodiesel as a commercial fuel is subject to a number of standards and regulations, some common to conventional diesel and others specific to this type of biofuel.

One of the important specifications of biodiesel is related to its behaviour at low temperatures. It is important to know the temperature at which crystallization starts, known as the cloud point, CP (EN 23015, ASTM D-2500), the temperatures at which the fuel filters and lines become plugged, CFPP (EN 116, IP-309, ASTM D-6371), the low-temperature operability of the biodiesel, the biodiesel capacity to pass through an engine fuel filtration system that is determined by low temperature flow test, LTFT (ASTM D-4539) and the temperature at which the fluid gels, thwarting its flow, known as the Plugging Point, PP (ASTM D-97, ASTM D-5949) [1]. Since saturated fatty acid esters present high melting temperatures, at low ambient temperatures crystals of these compounds appear and, in this way, the storage, transport and principally the use of the biodiesel can be

compromised. This is also true when the use of blends of biodiesel with conventional diesel are considered [2].

The composition of biodiesel in fatty esters is closely related to the oil or fat used as the raw material, and generally two or three fatty esters are responsible for more than 80% of the total biodiesel composition [1]. In this way a binary mixture of FAEE containing ethyl palmitate could represent, in a simplified way, a palm biodiesel produced from palm oil that can easily be produced in the north and northeast of Brazil. Interest in determining the ethylic biodiesel properties was driven by the Brazilian capacity for ethanol production from sugar cane, and because ethanol, contrary to methanol, is obtained from a renewable source. The biodiesel produced by esterification with ethanol remains a carbon neutral molecule, whilst that esterified with methanol does not, implying in a 5% loss in carbon neutrality, which is a significant value to the environment [3]. Moreover, Brazil has an installed production capacity of several million litres of ethanol per day from sugar cane. The data here presented is important to the biodiesel production via the ethylic route and also to the knowledge of the low temperatures properties of ethylic biodiesel.

### 2. Experimental section

In this study was determined the saturation lines, corresponding to the cloud points, of binary mixtures of ethyl palmitate with ethyl caprylate, ethyl caprate, ethyl laurate, ethyl myristate, ethyl oleate and ethyl linoleate using a Differential Scanning Calorimetry (DSC).

\* Corresponding author. Tel.: +55 19 3251 4037; fax: +55 19 3251 4027.

E-mail addresses: [mcdcosta@yahoo.com.br](mailto:mcdcosta@yahoo.com.br) (M.C. Costa), [laslorboros@hotmail.com](mailto:laslorboros@hotmail.com) (L.A.D. Boros), [batista.m@ua.pt](mailto:batista.m@ua.pt) (M.L.S. Batista), [jc Coutinho@ua.pt](mailto:jc Coutinho@ua.pt) (J.A.P. Coutinho), [mak@feq.unicamp.br](mailto:mak@feq.unicamp.br) (M.A. Krähenbühl), [tomze@fea.unicamp.br](mailto:tomze@fea.unicamp.br) (A.J.A. Meirelles).

The DSC was calibrated using indium (99.999%), certified by TA Instruments, cyclohexane (min 99.9%) and naphthalene (min 99%), both supplied by Merck. The high purity fatty acid esters (min 99%), obtained from Nu-Chek, were used with no further purification. The mixtures were prepared by weighing on an analytical balance with a precision of  $\pm 0.2$  mg, and the amounts weighed placed in a glass tube and heated in an atmosphere of nitrogen with constant stirring to a temperature 10 K above the highest melting point of the pure components.

A TA Instruments MDSC 2920 calorimeter, equipped with a refrigerated cooling system and operating between 203 and 600 K, was used to obtain the experimental data. Small amounts of each mixture (2–5 mg) were weighed on a microanalytical balance (Perkin–Elmer AD6) with an accuracy of  $\pm 0.2 \times 10^{-5}$  mg, and sealed in aluminium pans. The experimental data were collected after a pre-treatment of the samples inside the DSC cell, as described in a previous study [4–6].

The accuracy of the experimental melting points of the mixtures was evaluated on the basis of repeated runs performed with the calibration substances and some mixtures. The experimental deviations were estimated to be no higher than 0.3 K [6].

### 3. Modelling

Equations of State (EoS) are often used for correlating phase equilibrium in fatty systems [7,8]. In the present study the Soave–Redlich–Kwong EoS [9] was used to describe the crystallization/melting behaviour of fatty acid ethyl esters. The approach used here was previously proposed by the same authors for alkane mixtures [10–23], and was also successfully applied to fatty acids [5] and fatty acid methyl esters [24].

The solid–liquid equilibrium is established by equality of the fugacity of each component in the liquid and solid phases

$$f_i^L(T, P, x_i^L) = f_i^S(T, P, x_i^S) \quad (1)$$

The liquid phase fugacity can be obtained from

$$f_i^L(T, P, x_i^L) = P x_i^L \phi_i^L \quad (2)$$

where the fugacity coefficient  $\phi_i^L$  is calculated using the Soave–Redlich–Kwong EoS [9] with the LVM mixing rules [25,26]. The volumetric properties calculated by the cubic EoS are corrected using the volume translation proposed by Peneloux et al. [27].

The solid-phase fugacity at a pressure  $P$  is obtained from

$$\ln f_i^S(P) = \ln f_i^S(P_0) + \frac{1}{RT} \int_{P_0}^P \bar{v}_i^S dP \quad (3)$$

where the fugacity of the component  $i$  in the solid phase at reference pressure  $P_0$ , here taken as the atmospheric pressure, is calculated from its fugacity in the sub-cooled liquid state at the same temperature  $T$ .

$$f_i^S(P_0) = x_i^S \gamma_i^S(P_0) f_i^{0,L}(P_0) \exp \left[ -\frac{\Delta_{fus} H_i}{RT} \left( 1 - \frac{T}{T_{fus,i}} \right) \right] \quad (4)$$

where  $\gamma_i^S$  represents the activity coefficient of the compound  $i$  in the solid phase and  $T_{fus,i}$  and  $\Delta_{fus} H_i$  are, respectively, the fusion temperature and enthalpy of fusion of the pure compound  $i$  at the reference pressure. Since the systems studied in this work were measured at atmospheric pressure, the Poynting correction term in Eq. (3) can be neglected and Eq. (3) can be written as

$$f_i^S(T, P, x_i^S) = x_i^S \gamma_i^S(T, P_0, x_i^S) f_i^{0,L}(T, P_0) \exp \left[ -\frac{\Delta_{fus} H_i}{RT} \left( 1 - \frac{T}{T_{fus,i}} \right) \right] \quad (5)$$

The activity coefficients  $\gamma_i^S$  of the solid phase were described by means of the new version of the predictive UNIQUAC model [13,14]. The predictive UNIQUAC model can be written as

$$\frac{g^E}{RT} = \sum_{i=1}^n x_i \ln \left( \frac{\Phi_i}{x_i} \right) + \frac{Z}{2} \sum_{i=1}^n q_i x_i \ln \left( \frac{\theta_i}{\Phi_i} \right) - \sum_{i=1}^n x_i q_i \times \ln \left[ \sum_{j=1}^n \theta_j \exp \left( -\frac{\lambda_{ij} - \lambda_{ii}}{q_i RT} \right) \right] \quad (6)$$

with

$$\theta_i = \frac{x_i q_i}{\sum_j x_j q_j} \quad \text{and} \quad \Phi_i = \frac{x_i r_i}{\sum_j x_j r_j} \quad (7)$$

The predictive local composition concept [28–32] allows for estimation of the interaction energies ( $\lambda_{ij}$ ) used by this model, without fitting to the experimental data. The pair interaction energies between two identical molecules are estimated from the enthalpy of sublimation of the pure crystalline component

$$\lambda_{ii} = -\frac{2}{Z} (\Delta_{sub} H_i - RT) \quad (8)$$

where  $Z = 10$  is the coordination number. The enthalpies of sublimation ( $\Delta_{sub} H = \Delta_{vap} H + \Delta_{fus} H$ ) are calculated at the melting temperature of the pure component.

The pair interaction energy between two non-identical molecules is given by

$$\lambda_{ij} = \lambda_{ji} = \lambda_{ii} \quad (9)$$

where  $i$  is the compound with the shorter alkyl chain of the pair  $ij$ .

As an alternative, a simpler approach for the description of the *solidus* line measured in this study was also tested. It was assumed that the solid phase formed was essentially a pure fatty ester, and that the liquid phase was ideal. Based on these assumptions the relation between the composition of the mixture,  $x_i$ , and the melting/cloud point,  $T$ , was given by the classical solid–liquid equilibrium equation.

$$x_i^L = \exp \left[ -\left( \frac{\Delta_{fus} H_i}{R} \left( \frac{1}{T} - \frac{1}{T_{fus,i}} \right) \right) \right] \quad (10)$$

The solid–liquid equilibrium models, adopted here, are predictive models that only use pure component properties to calculate the behaviour of the phase. Correlations for the thermophysical properties of fatty acid esters were proposed in a previous paper [33]. The most adequate estimates for the critical temperature ( $T_c$ ) and pressure ( $P_c$ ) of saturated ethyl esters are obtained using the Nikitin et al. [34] correlation. For the acentric factor ( $\omega$ ), the Hang and Peng [35] model was found to be the most adequate. The values used in this work are reported in Table 1.

The melting temperatures ( $T_{fus}$ ) of the saturated and unsaturated ethyl esters were obtained directly from the experimental thermograms.

The correlations used for the estimation of the fusion ( $\Delta_{fus} H$ ) and vapourisation enthalpies ( $\Delta_{vap} H$ ) of the saturated ethyl esters were, respectively [33]

$$\Delta_{fus} H = 3.92C_n + 16.80 \quad (11)$$

$$\Delta_{vap} H = 4.9C_n + 9.0 \quad (12)$$

where the enthalpies are expressed in  $\text{kJ} \times \text{mol}^{-1}$ . For the unsaturated ethyl esters it was assumed that the differences between the fusion ( $\Delta_{fus} H$ ) and vapourisation ( $\Delta_{vap} H$ ) enthalpies of the saturated and unsaturated ethyl esters would be the same as those observed for the methyl esters [33].

### 4. Results and discussion

The melting points of binary mixtures of ethyl palmitate, an ethyl ester found in large quantities in the biodiesel produced from palm oil by the ethylic route, with ethyl caprylate, ethyl caprate,

**Table 1**  
Thermophysical properties used for the ethyl esters studied in this work.

Fatty ester		$T_c$ (K)	$P_c$ (bar)	$\omega$	$\Delta_{vap}H$ (kJ mol <sup>-1</sup> )	$\Delta_{fus}H$ (kJ mol <sup>-1</sup> )	$T_{fus}$ (K)
Ethyl caprylate	C <sub>10:0</sub>	656.39	21.60	0.628	58.0	22.40	230.35
Ethyl caprate	C <sub>12:0</sub>	690.216	18.46	0.709	67.8	30.23	254.51
Ethyl laurate	C <sub>14:0</sub>	719.13	15.97	0.787	77.6	38.07	272.59
Ethyl myristate	C <sub>16:0</sub>	744.27	14.02	0.862	87.4	45.91	287.37
Ethyl palmitate	C <sub>18:0</sub>	766.41	12.43	0.935	97.2	53.75	297.69
Ethyl oleate	C <sub>20:1</sub>	771.07	11.12	1.013	107.3	25.39	255.12
Ethyl linoleate	C <sub>20:2</sub>	785.89	11.57	1.008	108.9	24.39	217.94

ethyl laurate, ethyl myristate, ethyl oleate and ethyl linoleate were measured by DSC. The results obtained with ethyl stearate were reported in a previous paper [4]. These fatty esters can be found in small quantities in palm oil biodiesel and also in biodiesel from other vegetable and animal oils and fats.

Tables 2 and 3 show the experimental data obtained for the saturation lines of each system studied here. The data show that the systems with ethyl laurate and ethyl myristate present a eutectic point. Although probably present in other systems at concentrations very close to being pure compounds, a clear eutectic point is only perceptible for systems in which the difference in melting points of the pure esters is smaller than 30 K.

Figs. 1 and 2 show the phase diagrams of the mixtures studied, presenting behaviour similar to that found for the binary systems formed with ethyl stearate. The heavy ester controls the melting points of the mixture, and the introduction of a second ethyl ester with a lower melting point does not induce a significant decrease in the melting/cloud point of the mixtures up to concentrations of 50 mol%. Also the phase diagrams of the various esters did not present significant differences between them up to the eutectic point.

In the present study, only the saturation lines for these systems were reported. However, as observed for previously studied binary mixtures of saturated fatty acids [36–38], below the saturation line the phase diagram is not as deceptively simple as the results here reported could indicate. In fact the DSC thermograms indicated that the solid phase behaviour of the binary mixtures of saturated fatty esters could be as complex as that observed for the binary mixtures of fatty acids. This subject is still under investigation and will be the object of a future study.

The predictive UNIQUAC model proposed for the prediction of the cloud points of diesels and crude oils [9,13,14,16–23, 25,26,33,39], and successfully applied to fatty acid, methyl and ethyl esters [4,6] and to the low temperature behaviour of biodiesels [40], was used to describe the experimental data measured in the present study. The full lines shown in Figs. 1 and 2 were generated by the predictive UNIQUAC model. The average deviation obtained between the experimental and calculated data was inferior to 0.5 K, even for systems formed with ethyl oleate and linoleate,

**Table 2**  
Melting points of the binary systems of saturated ethyl esters with ethyl palmitate.

Ethyl caprylate + ethyl palmitate		Ethyl caprate + ethyl palmitate		Ethyl laurate + ethyl palmitate		Ethyl myristate + palmitate	
$x_{C10:0}$	$T$ (K)	$x_{C12:0}$	$T$ (K)	$x_{C14:0}$	$T$ (K)	$x_{C16:0}$	$T$ (K)
0.0000	297.69	0.0000	297.69	0.0000	297.69	0.0000	297.69
0.1163	296.69	0.1595	296.02	0.1331	296.48	0.0992	296.61
0.2028	295.61	0.2280	295.46	0.1828	295.33	0.1876	294.91
0.2918	294.53	0.3318	293.82	0.2871	293.18	0.2875	292.73
0.3923	292.13	0.4192	291.30	0.3906	292.23	0.3680	291.14
0.4483	291.58	0.5203	289.14	0.5007	290.12	0.4886	288.19
0.5558	289.68	0.6107	287.44	0.5965	287.42	0.5843	285.36
0.7126	282.21	0.6875	284.91	0.6904	282.32	0.6877	283.50
0.8201	277.10	0.7895	280.72	0.7760	279.11	0.7995	282.87
0.9359	265.56	0.9039	269.58	0.8652	268.69	0.8863	284.01
1.0000	228.19	1.0000	254.51	1.0000	272.59	1.0000	285.74

**Table 3**  
Melting points of the binary systems of unsaturated ethyl esters with ethyl palmitate.

Ethyl palmitate + ethyl oleate		Ethyl palmitate + ethyl linoleate	
$x_{C20:1}$	$T$ (K)	$x_{C20:2}$	$T$ (K)
0.0000	297.69	0.0000	297.69
0.0975	297.41	0.1062	297.25
0.2018	295.85	0.2103	295.97
0.2852	294.54	0.2720	294.97
0.3918	294.00	0.3597	292.64
0.4975	290.33	0.4982	290.32
0.6033	287.29	0.5940	286.92
0.7157	283.29	0.7095	284.25
0.8251	276.26	0.8127	279.12
0.8927	271.81	0.9021	272.33
1.0000	254.67	1.0000	220.68

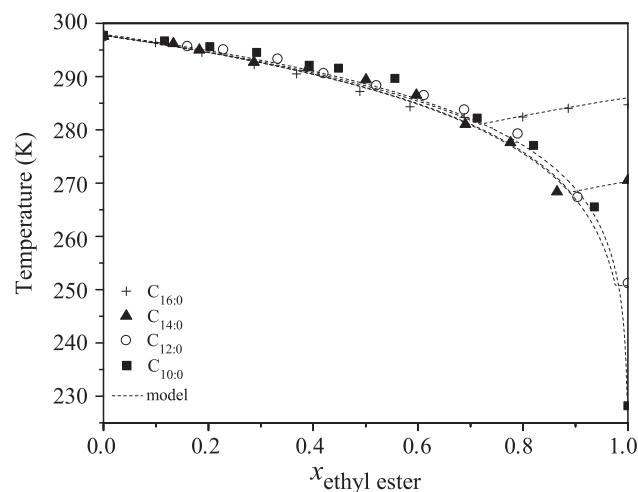


**Fig. 1.** Experimental and predicted melting points of the binary mixtures of ethyl caprylate, ethyl caprate, ethyl laurate or ethyl myristate with ethyl palmitate.

showing that the model describes the experimental data very well. This confirms the ability of the model to describe the low temperature behaviour of fatty ester mixtures.

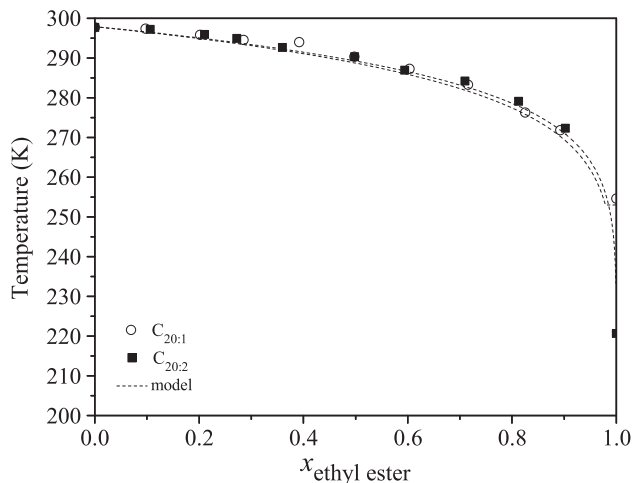


Fig. 2. Experimental and predicted melting points of the binary mixtures of ethyl oleate or ethyl linoleate with ethyl palmitate.

An alternative and simpler approach to the description of these data was also attempted here, assuming an ideal mixture in the liquid phase and a pure solid phase. The relationships between the melting temperature of the mixture,  $T$ , and its composition,  $x$ , are given by Eq. (10). This approach is also predictive as the fitting of no parameters is required to describe the experimental data, and only the melting temperatures and enthalpies of the pure compounds are required to use the model. The results obtained, reported in Figs. 1 and 2 as dashed lines, are surprisingly good, and essentially identical to those obtained using the more complex approach based on the predictive UNIQUAC model. The limitations of this simple approach for the description of real biodiesel were highlighted and discussed in a previous work [40].

## 5. Conclusion

Six binary mixtures of ethyl palmitate with saturated and unsaturated fatty acid ethyl esters were studied by DSC. The experimental phase diagrams for these binary systems are reported here. The data indicated that the cloud points of the mixtures were essentially controlled by the fatty ester with higher melting temperature when this one was present in concentrations above 50 mol%.

It was shown that the predictive UNIQUAC model was able to produce an excellent prediction of the experimental data measured in this work, and that a simple ideal solution model can describe the melting points for these simple systems with an accuracy similar to that of the predictive UNIQUAC model.

## Acknowledgments

The authors are grateful to CNPq (304495/2010-7 and 480992/2009-6), FAPESP (08/09502-0 and 08/56258-8), and FAPEX/UNICAMP for their financial support.

## References

- [1] Imahara H, Minami E, Saka S. Thermodynamic study on cloud point of biodiesel with its fatty acid composition. *Fuel* 2006;85:1666–70.
- [2] Joshi RM, Pegg MJ. Flow properties of biodiesel fuel blends at low temperatures. *Fuel* 2007;86:143–51.
- [3] Jones JC. On the use of ethanol in the processing of biodiesel fuels. *Fuel* 2010;89:1183.
- [4] Boros L, Batista MLS, Vaz RV, Figueiredo BR, Fernandes VFS, Costa MC, et al. Crystallization behavior of mixtures of fatty acid ethyl esters with ethyl stearate. *Energy Fuels* 2009;23:4625–9.

- [5] Costa MC, Krähenbühl MA, Meirelles AJA, Daridon JL, Pauly J, Coutinho JAP. High pressure solid–liquid equilibria of fatty acids. *Fluid Phase Equilib* 2007;253:118–23.
- [6] Costa MC, Rolemberg MP, Boros LAD, Krähenbühl MA, Oliveira MG, Meirelles AJA. Solid–liquid equilibrium of binary fatty acids mixtures. *J Chem Eng Data* 2007;52:30–6.
- [7] Comim SRR, Franceschi E, Borges GR, Corazza ML, Oliveira JV, Ferreira SRS. Phase equilibrium measurements and modelling of ternary system (carbon dioxide plus ethanol plus palmitic acid). *J Chem Thermodyn* 2010;42:348–54.
- [8] Ndiaye PM, Franceschi E, Oliveira D, Dariva C, Tavares FW, Oliveira JV. Phase behavior of soybean oil, castor oil and their fatty acid ethyl esters in carbon dioxide at high pressures. *J Supercrit Fluids* 2006;37:29–37.
- [9] Soave G. Equilibrium constants from a modified Redlich–Kwong equation of state. *Chem Eng Sci* 1972;27:1197–972.
- [10] Pauly J, Daridon JL, Coutinho JAP, Dirand M. Crystallisation of a multiparaffinic wax in normal tetradecane under high pressure. *Fuel* 2005;84:453–9.
- [11] Sansot JM, Pauly J, Daridon JL, Coutinho JAP. Modeling high-pressure wax formation in petroleum fluids. *AIChE J* 2005;51:2089–97.
- [12] Coutinho JAP, Gonçalves C, Marrucho IM, Pauly J, Daridon JL. Paraffin crystallization in synthetic mixtures: predictive local composition models revisited. *Fluid Phase Equilib* 2005;233:28–33.
- [13] Coutinho JAP, Mirante F, Pauly J. A new predictive UNIQUAC for modeling of wax formation in hydrocarbon fluids. *Fluid Phase Equilib* 2006;247:8–17.
- [14] Coutinho JAP, Dauphin C, Daridon JL. Measurements and modelling of wax formation in diesel fuels. *Fuel* 2000;79:607–16.
- [15] Coutinho JAP. A thermodynamic model for predicting wax formation in jet and diesel fuels. *Energy Fuels* 2000;14:625–31.
- [16] Coutinho JAP, Daridon JL. Low-pressure modeling of wax formation in crude oils. *Energy Fuels* 2001;15:1454–60.
- [17] Daridon JL, Pauly J, Coutinho JAP, Montel F. Solid–liquid–vapor phase boundary of a North Sea waxy crude: measurement and modeling. *Energy Fuels* 2001;15:730–5.
- [18] Pauly J, Daridon JL, Coutinho JAP. Measurement and prediction of temperature and pressure effect on wax content in a partially frozen paraffinic system. *Fluid Phase Equilib* 2001;187:71–82.
- [19] Mirante FIC, Coutinho JAP. Cloud point prediction of fuels and fuel blends. *Fluid Phase Equilib* 2001;180:247–55.
- [20] Queimada AJN, Dauphin C, Marrucho IM, Coutinho JAP. Low temperature behaviour of refined products from DSC measurements and their thermodynamical modelling. *Thermochim Acta* 2001;372:93–101.
- [21] Coutinho JAP, Mirante F, Ribeiro JC, Sansot JM, Daridon JL. Cloud and pour points in fuel blends. *Fuel* 2002;81:963–7.
- [22] Pauly J, Daridon JL, Sansot JM, Coutinho JAP. The pressure effect on the wax formation in diesel fuel. *Fuel* 2003;82:595–601.
- [23] Coutinho JAP, Edmonds B, Moorwood T, Szczepanski R, Zhang XH. Reliable wax predictions for flow assurance. *Energy Fuels* 2006;20:1081–8.
- [24] MacNaughtan W, Farhat IA, Himawan C, Starov VM, Stapley AGF. A differential scanning calorimetry study of the crystallization kinetics of tristearin–tripalmitin mixtures. *J Am Oil Chem Soc* 2006;83:1–9.
- [25] Boukouvalas C, Spiliotis N, Coutsikos P, Tzouvaras N, Tassios D. Prediction of vapor–liquid–equilibrium with the Lcvm model – a linear combination of the Vidal and Michelsen Mixing rules coupled with the original Unifac and the T-Mpr equation of state. *Fluid Phase Equilib* 1994;92:75–106.
- [26] Boukouvalas CJ, Magoulas KG, Stamataki SK, Tassios DP. Prediction of vapor–liquid equilibria with the Lcvm model: systems containing light gases with medium and high molecular weight compounds. *Ind Eng Chem Res* 1997;36:5454–60.
- [27] Peneloux A, Rauzy E, Freze R. A consistent correction for Redlich–Kwong–Soave volumes. *Fluid Phase Equilib* 1982;8:7–23.
- [28] Coutinho JAP, Knudsen K, Andersen SI, Stenby EH. A local composition model for paraffinic solid solutions. *Chem Eng Sci* 1996;51:3273–82.
- [29] Coutinho JAP, Stenby EH. Predictive local composition models for solid/liquid equilibrium in  $n$ -alkane systems: Wilson equation for multicomponent systems. *Ind Eng Chem Res* 1996;35:918–25.
- [30] Coutinho JAP. Predictive UNIQUAC: a new model for the description of multiphase solid–liquid equilibria in complex hydrocarbon mixtures. *Ind Eng Chem Res* 1998;37:4870–5.
- [31] Coutinho JAP, RuffierMeray V. Experimental measurements and thermodynamic modeling of paraffinic wax formation in undercooled solutions. *Ind Eng Chem Res* 1997;36:4977–83.
- [32] Coutinho JAP. Predictive local composition models: NRTL and UNIQUAC and their application to model solid–liquid equilibrium of  $n$ -alkanes. *Fluid Phase Equilib* 1999;160:447–57.
- [33] Lopes JCA, Boros L, Krahenbuhl MA, Meirelles AJA, Daridon JL, Pauly J, et al. Prediction of cloud points of biodiesel. *Energy Fuels* 2008;22:747–52.
- [34] Nikitin ED, Pavlov PA, Bogatishcheva NS. Critical properties of long-chain substances from the hypothesis of functional self-similarity. *Fluid Phase Equilib* 2005;235:1–6.
- [35] Han BX, Peng DY. A group-contribution correlation for predicting the centric factors of organic-compounds. *Can J Chem Eng* 1993;71:332–4.
- [36] Costa MC, Rolemberg MP, Meirelles AJA, Coutinho JAP, Krahenbuhl MA. The solid–liquid phase diagrams of binary mixtures of even saturated fatty acids differing by six carbon atoms. *Thermochim Acta* 2009;496:30–7.

- [37] Costa MC, Sardo M, Rolemberg MP, Coutinho JAP, Meirelles AJA, Ribeiro-Claro P, et al. The solid–liquid phase diagrams of binary mixtures of consecutive, even saturated fatty acids. *Chem Phys Lipids* 2009;160:85–97.
- [38] Costa MC, Sardo M, Rolemberg MP, Coutinho JAP, Meirelles AJA, Ribeiro-Claro P, et al. The solid–liquid phase diagrams of binary mixtures of consecutive, even saturated fatty acids: differing by four carbon atoms. *Chem Phys Lipids* 2009;157:40–50.
- [39] Coutinho JAP. A thermodynamic model for predicting wax formation in jet and diesel fuels. *Energy Fuels* 2000;14:625–31.
- [40] Coutinho JAP, Goncalves M, Pratas MJ, Batista MLS, Fernandes VFS, Pauly J, et al. Measurement and modeling of biodiesel cold-flow properties. *Energy Fuels* 2010;24:2667–74.